MATERIAL MODELING IN FINITE ELEMENT ANALYSIS

SECOND EDITION

Zhaochun Yang

CRC Press
Taylor & Francis Group

Material Modeling in Finite Element Analysis

Finite element analysis has been widely applied in mechanical, civil, and biomedical designs. This new edition provides the readers with comprehensive views of various material models through practical examples, which will help them better understand various materials and build appropriate material models in finite element analysis. *Material Modeling in Finite Element Analysis*, Second Edition, consists of four main parts: (1) metals, (2) polymers, (3) soils, and (4) modern materials. Each part starts with the structure and function of different materials and then follows the corresponding material models and the temperature and time effects on the material models. The final part focuses on user subroutines such as UserMat and UserHyper. This book presents some specific problems including the metal-forming process, combustion room, Mullins effect of rubber tires, viscoelasticity of liver soft tissues, small punch test, tunnel excavation, slope stability, concrete slump test, orthodontic wire, and piezoelectric microaccelerometer. All modeling files are provided in the appendices of this book. This book would be helpful for graduate students and researchers in the mechanical, civil, and biomedical fields who conduct finite element analysis. This book provides all readers with a comprehensive understanding of modeling various materials.

Zhaochun Yang received his PhD in Mechanical Engineering from the University of Pittsburgh in 2004. Since 2005, he has worked for big companies and national labs such as Nation Energy Technology Laboratory. He has been in the field of finite element analysis for over 20 years and has gained much experience, especially in material modeling. Up to now, he has published 12 journal papers and 3 books.

Material Modeling in Finite Element Analysis

Second Edition

Zhaochun Yang

CRC Press
Taylor & Francis Group
Boca Raton London New York

CRC Press is an imprint of the
Taylor & Francis Group, an **informa** business

Designed cover image © 123RF

Second edition published 2024
by CRC Press
2385 NW Executive Center Drive, Suite 320, Boca Raton FL 33431

and by CRC Press
4 Park Square, Milton Park, Abingdon, Oxon, OX14 4RN

CRC Press is an imprint of Taylor & Francis Group, LLC

First edition published by Taylor and Francis 2019

ISBN: 978-1-032-56602-3 (hbk)
ISBN: 978-1-032-56603-0 (pbk)
ISBN: 978-1-003-43631-7 (ebk)

DOI: 10.1201/9781003436317

Typeset in Times
by codeMantra

Contents

PART II Polymers

PART III Soil

PART IV Modern Materials

PART V Retrospective

Preface

Three years ago, inspired by the success of my first book, *Finite Element Analysis for Biomedical Engineering Applications*, I finished my second book, *Material Modeling in Finite Element Analysis,* to summarize my experience in material modeling. Soon after the second book was published, I questioned my decision to write and publish it because material modeling is a huge field and I only know a tiny part of it. Therefore, I devoted the past 3 years to studying material modeling to develop a deeper understanding of it. I also realized that more and more parts of the second book should be rewritten. Thus, in the past 2 months, I collected all materials and rewrote a new version of my book, *Material Modeling in Finite Element Analysis.* The major modifications include:

1. Reorganization of Part I in order of the material models, effect of time and temperature on material properties, and user subroutine;
2. Rewriting of user subroutines, UserMat and UserHyper, because they are the most important user material subroutines;
3. Clarification of the differences between the materials, such as Drucker-Prager vs Mohr-Coulomb, BISO vs BKIN, and creep vs viscoplasticity; and
4. Deletion of some unnecessary examples and addition of more practical problems, including the strain-hardening model, Veronda-Westman model, small punch test, and breast tumor model. Some typical problems, such as soil excavation, concrete slump test, and one-dimensional Terzaghi's problem, to help understand the geomechanics models are also included.

During the writing and publication of the new version of the book, I received help from many of my friends: Frank Marx, Dr. J.S. Lin, Dr. Jobie Gerken, Dr. Adi Adumitroaie, Dr. Rachmadian Wulandana, Dr. Zhi-Hong Mao, Dr. Krystyna Gielo-Perczak, Dr. Rika Carlsen, and Ronna Edelstein. Without their help, I could not have completed my revision process. I also greatly appreciate editor Marc Gutierrez, editorial assistant Kianna Delly, and other staffs of CRC Press for their assistance in publishing this book. Finally, I welcome any feedback for improving this book.

1 Introduction

We live in a modern world of buildings, cars, airplanes, and medical advances, including coronary angioplasty. Buildings require structural analysis from civil engineers, while the manufacture of cars and airplanes depends on strong mechanical design. Biomedical engineering plays a significant role in coronary surgeries. All these fields demand an understanding of the stress state of the structures. With the development of computer technology, finite element analysis has been widely used in these fields. Specifically, since the 1970s, many commercial finite element software companies have evolved: ANSYS, ABAQUS, COMSOL, ADINA, LS-DYNA, and MARC. Among these, ANSYS emerges as the leader.

One of the key processes in finite element analysis is building material models. The structural analysis of a building is associated with soils; the manufacture of a car involves metals; the airplane has many components made of composites to ensure both high strength and low weight; and the stent in the coronary angioplasty is made of shape memory alloys. When we create finite element models to conduct stress analysis for their designs, we must adopt a variety of material models corresponding to different materials, because under the same geometry and loadings and boundary conditions, different materials may have unique behaviors. For example, it is hard to pull a steel rod, but the same force can easily deform a rubber rod. If we pull the metal rod to plasticity, the plastic strains remain after the force is gone. However, when the metal rod is made of shape memory alloys, the remaining transformation strains can be removed with the rise of temperature. Unlike these materials, the soil has little resistance to tension. The purpose of this book is to acknowledge that different materials have unique features and to present readers with a comprehensive view of various material models. By providing practical examples, this book will enable readers to better understand the material models, how to select appropriate material models, and how to define the correct solution set in the finite element analysis of complicated engineering problems. As discussed above, ANSYS is the leading software in the field of finite element analysis. Thus, the examples in this book are provided in the form of ANSYS input files, which makes it convenient for the readers to learn and practice these examples.

This book consists of four main parts. After the introductory chapter, the first part focuses on metals and alloys. Chapter 2 introduces the structure of alloys and their mechanical features. Some plastic models such as the isotropic hardening, kinematic hardening, and Chaboche model, along with ratcheting simulation, are presented in Chapter 3. Chapter 4 discusses the material properties, including viscoplasticity and creep, as a function of time. As the material properties of metals are temperature-dependent, Chapter 5 examines the influence of temperature on a combustion chamber. The last chapter in Part I shows how to develop UserMat and offers the strain-hardening model as an example.

DOI: 10.1201/9781003436317-1

The second part discusses polymers. After Chapter 7 depicts the structure and material properties of polymers, Chapter 8 presents some hyperelastic material models and curve-fitting of the models' material parameters. The viscoelasticity of elastomers and the shift functions are discussed in Chapter 9. Chapter 10 introduces eight chain-based viscoplasticity models, including application of the Bergstrom-Boyce model for simulation of the small punch test. The stress responses of elastomers always experience softening during the first few loading cycles. That is regarded as a damage accumulation in the material, which refers to the Mullins effect of elastomers; Chapter 11 focuses on this and includes an example of a rubber tire. UserHyper is available in ANSYS for customers to create their own hyperelastic models. Chapter 12 presents one example of UserHyper to reproduce the Veronda-Westman model.

Soils are the topic of the third part. Chapter 13 introduces the structure and various classifications of soils. Four major material models of soils—the Cam Clay model, Drucker-Prager model, Mohr-Coulomb model, and Jointed Rock model—are discussed in Chapters 14–17, respectively. These chapters also cover some typical and practical problems: excavation of the soil, a tower on the ground, a concrete slump test, soil-arch interaction, stability of a slope, and a tunnel excavation. Since soils are composed of rocks, water, and air, Chapter 18 explores the consolidation of soils and its application for simulation of the one-dimensional Terzaghi's problem and consolidation of rocks with three wells.

Part IV highlights modern materials. One widely used modern material is composite, which was developed in the 1950s due to the airplane design requiring high strength and low weight. Structure and material properties of composites are presented in the first part of Chapter 19, followed by an application on an adapter in flight-qualification testing and crack growth in the single-leg bending problem.

Chapter 20 examines functionally graded materials and their simulation in ANSYS using TBFIELD technology.

The unique features of shape memory alloys (SMAs), superelasticity, and shape memory effect are discussed in Chapter 21. The chapter includes two examples to demonstrate SMAs' applications: (1) orthodontic wire using the superelasticity feature and (2) a vacuum-tight shape memory flange using shape memory effect.

Chapter 22 reviews the structure and mechanical behavior of piezoelectric materials. This is followed by the simulation of a thin-film piezoelectric microaccelerometer using the piezoelectric material model in ANSYS.

Nanoscale materials refer to a group of substances with at least one dimension less than approximately 100 nm that attract more and more interest. The first part of Chapter 23 introduces nanoscale materials; in the second part, Young's modulus of nano-Fe particles is determined from the experimental data of a ball made of Fe particles using the optimization algorithm in ANSYS.

Chapter 24 reviews the features of metals/alloys, polymers, soils, and modern materials and discusses the relation between material properties and structures, as well as the relation between temperature and material properties. It also examines the solution control for various materials.

Part I

Metal

Metal plays a dominant role in modern industry, especially in the manufacturing of cars, airplanes, and ships. Its mechanical design requires a clear understanding of its stress and strain states. Therefore, Part I focuses on many metal material models implemented in ANSYS.

Chapter 2 introduces the structure and material properties of metal. Some plastic models, including the isotropic hardening and kinematic hardening models, are discussed in Chapter 3. Chapter 4 focuses on viscoplasticity and creep of the metal. The influence of temperature on the material properties is analyzed in Chapter 5. User subroutine and implementation of the strain-hardening model are covered in Chapter 6.

DOI: 10.1201/9781003436317-2

2 Structure and Material Properties of Metal

Material properties of metal are closely linked with its structure. Thus, this chapter first presents the structure of metal and then gives the material properties of metal.

2.1 STRUCTURE OF METAL

A metal is a material in which the atoms are joined together by metallic bonds (see Figure 2.1). The delocalized electrons and the strong interaction forces between the positive atom nuclei give the metal features such as good thermal and electrical conduction.

Assuming the material's atoms as a perfect crystal, the bond energy is expressed as [1]

$$U = \frac{-ACe^2}{r} + \frac{B}{r^n} \tag{2.1}$$

where A, B, C, and e are material constants.

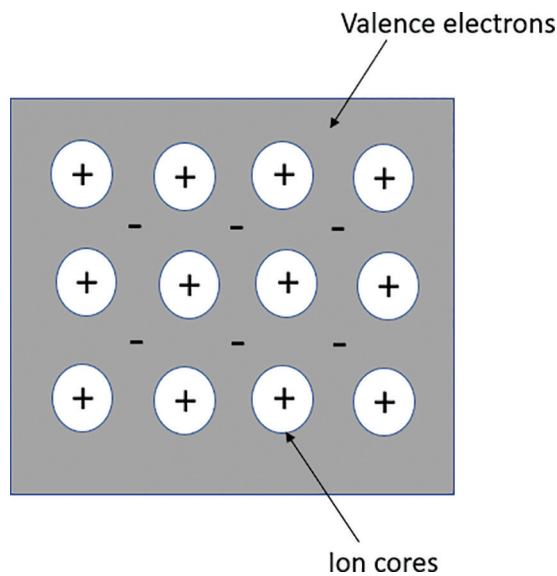

FIGURE 2.1 Atoms are held together by metallic bonds in a metal.

DOI: 10.1201/9781003436317-3

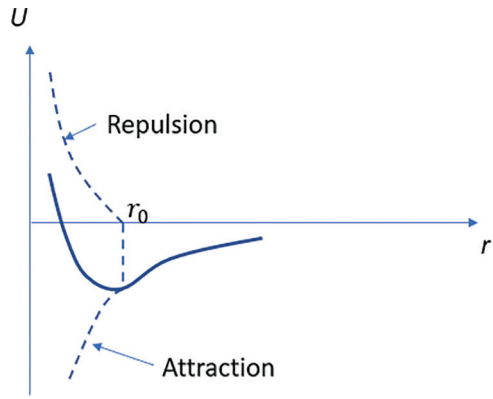

FIGURE 2.2 Bond energy function.

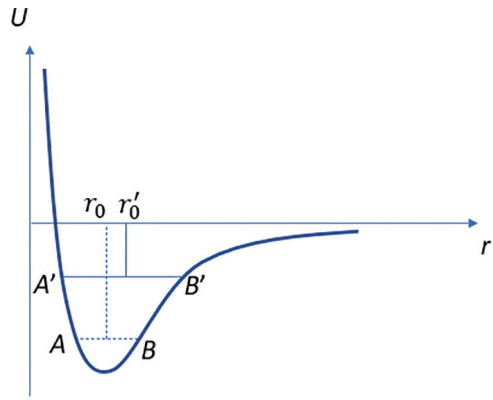

FIGURE 2.3 Anharmonicity of the bond energy function [1].

As shown in Figure 2.2, the curve is more flattened out at larger separation distances. When the distance between atoms is less than r_0, the forces between the atoms are repulsive. When the distance between atoms is greater than r_0, the forces become attractive.

Anharmonicity of the bond energy function explains why materials expand when the temperature increases (see Figure 2.3). As the internal energy rises due to the addition of heat, the system oscillates between the new positions marked *A*' and *B*' from the original positions *A* and *B*. Since the curve is not shaped like a sine curve, the new separation distance is longer than the previous one. Thus, the material has expanded, thereby causing the thermal strain.

2.2 ELASTICITY AND PLASTICITY OF METAL

When a force is applied to the metal, the layers of atoms start to roll over each other. If the force is released, the layers of atoms fall back to their original positions. Then, the metal is regarded as elastic (see Figure 2.4a).

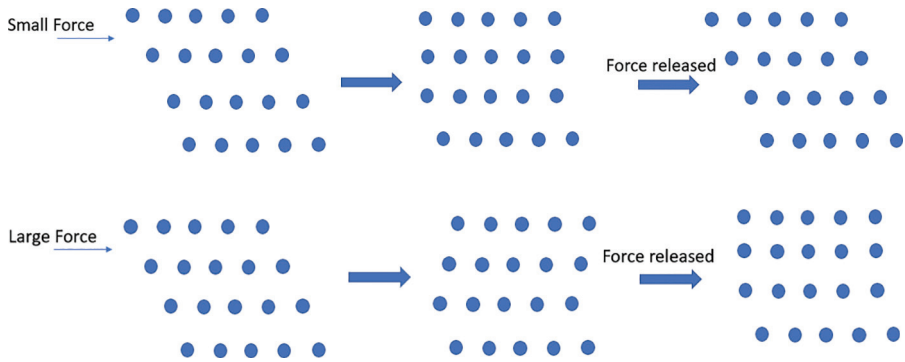

FIGURE 2.4 Illustration of a metal in elastic and plastic stages: (a) elastic stage and (b) plastic stage.

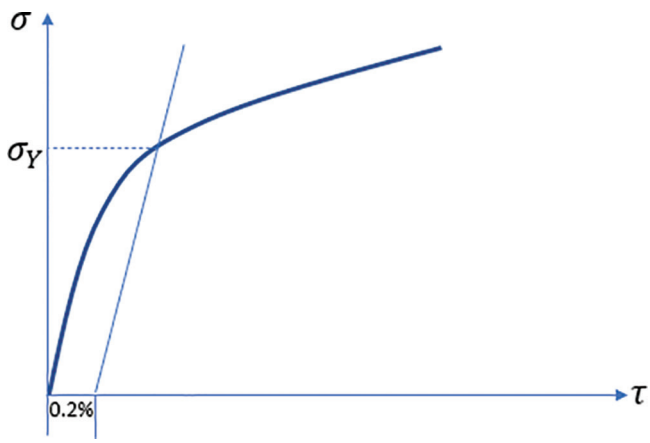

FIGURE 2.5 Stress-strain curve of the metal.

If the force is big enough that the atoms cannot fall back to their starting positions after the force is released, the metal is permanently changed (see Figure 2.4b).

Based on the above statements, the uniaxial tension tests of the metal show that when the stresses of the metal are below the yield stress σ_Y, the metal is elastic. When the stresses of the metal are higher than the yield stress σ_Y, the metal yields (see Figure 2.5). Yield driven by shearing stresses slides one plane along another (see Figure 2.6). The plastic deformation due to yield is a viscous flow process. Like flow in liquids, plastic flow has no volume change with Poisson's ratio $\upsilon = 0.5$.

Normally, if the material is in the elastic stage, it is not likely to fail. This is not true for brittle materials like ceramics because they fracture before they yield. However, for most of the structural materials, no damage occurs before yield. Thus, in the structural design, the materials required within the elastic stage use a safety factor. However, the plasticity of the metal has applications in industries such as metal forming. Therefore, some plastic models are introduced in Chapter 3.

FIGURE 2.6 Sliding is induced by shear stresses.

REFERENCE

1. Roylance, D., *Mechanical Properties of Materials*, MIT, Cambridge, 2008.

3 Some Plastic Material Models of Metals

After introducing the plasticity theory, Chapter 3 presents some isotropic hardening models and kinematic hardening models; it also includes a simulation of ratcheting in a notched bar.

3.1 INTRODUCTION OF PLASTICITY

The uniaxial tension test of the ductile material always has the typical stress-strain curve (see Figure 3.1), which shows the linear elasticity (*OA*), nonlinear elasticity (*AB*), the yield point *B*, the hardening stage from *B* to *D*, and the unloading stage *DE*. Figure 3.1 indicates that the total strain is composed of the elastic strain ε^{el} and plastic strain ε^{pl}:

$$\varepsilon = \varepsilon^{el} + \varepsilon^{pl} \tag{3.1}$$

The stress is determined by the elastic strain ε^{el}

$$\boldsymbol{\sigma} = \mathbf{D}\varepsilon^{el} \tag{3.2}$$

where **D** is the stiffness matrix.

The general yield function is expressed as

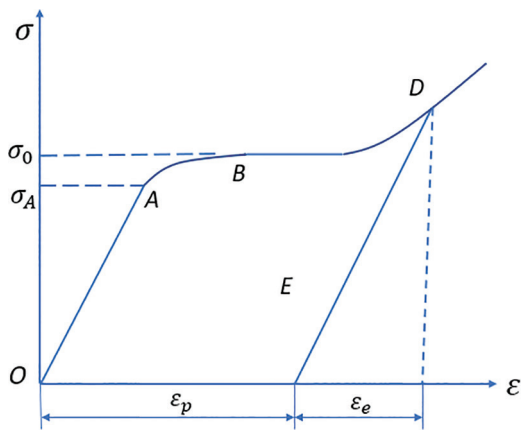

FIGURE 3.1 Stress-strain curve of the ductile material.

DOI: 10.1201/9781003436317-4

$$f(\boldsymbol{\sigma},\xi)=0 \tag{3.3}$$

where ξ refers to a set of internal variables.

When $f(\boldsymbol{\sigma},\xi)<0$, it is inside the yield surface and in an elastic state. No stresses exist outside the yield surface; instead, the stresses are either on or inside the yield surface.

Hardening occurs when an increase in stress leads to an increase in plastic strain. There are two types of hardening:

1. isotropic hardening of the yield surface (see Figure 3.2)

   The isotropic hardening changes the size of the yield surface but keeps the shape of the yield surface. It can model the behavior of the metals under monotonic loading. BISO and MISO in ANSYS belongs to isotropic hardening (see Figures 3.3 and 3.4), which can be defined by the following commands, respectively [1,2]:

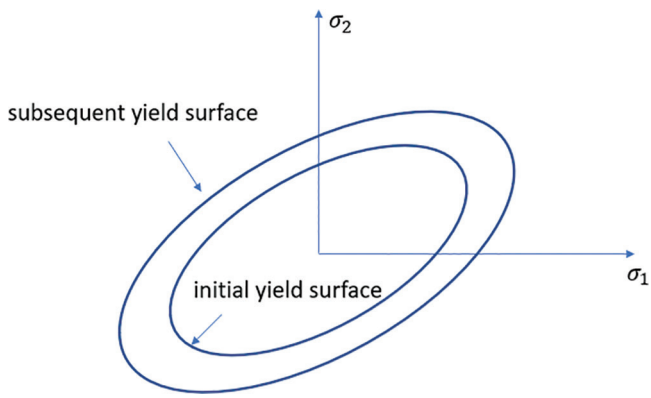

FIGURE 3.2 Isotropic hardening.

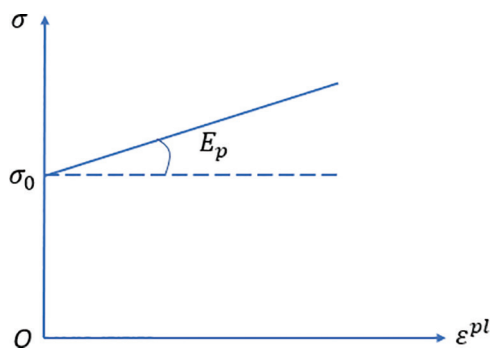

FIGURE 3.3 Plastic strain vs stress for bilinear isotropic hardening.

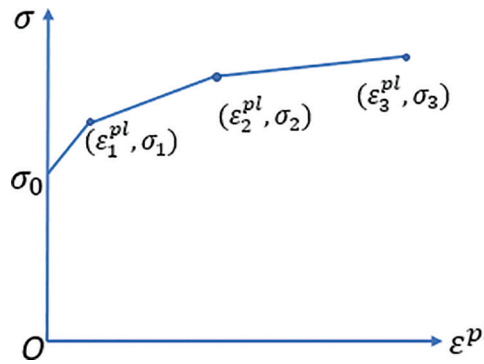

FIGURE 3.4 Plastic strain vs stress for multilinear isotropic hardening.

```
TB, Plastic, matid,BISO
TBDATA, 1, σ0, Ep
```

And

```
TB, Plastic, matid,MISO
TBPT, DEFI, 0, σ0
TBPT, DEFI, ε1pl, σ1
TBPT, DEFI, ε2pl, σ2
…
TBPT, DEFI, εipl, σi
```

2. kinematic hardening of the yield surface (see Figure 3.5)

   Kinematic hardening changes the shape of the yield surface, such as BKIN and KINH in ANSYS. Its yield criteria become

$$f(\boldsymbol{\sigma}-\boldsymbol{\alpha},\xi)=0 \tag{3.4}$$

   where α is the back stress that shifts the position of the yield surface in stress space during plastic deformation.

   Their definition in ANSYS is like that of BISO and MISO, respectively.

   Next, we conducted a uniaxial cyclic loading simulation to show the difference between isotropic hardening (BISO) and kinematic hardening (BKIN). The cyclic loading with time is illustrated in Figure 3.6, and the results (stress-strain curve) are presented in Figure 3.7; this clearly indicates that the BISO model increases yield surface, and the BKIN model only moves the yield surface center but does not change the size of the yield shape.

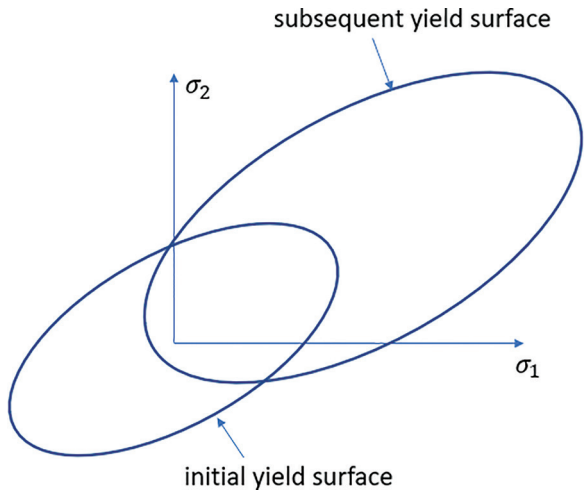

FIGURE 3.5 Kinematic hardening.

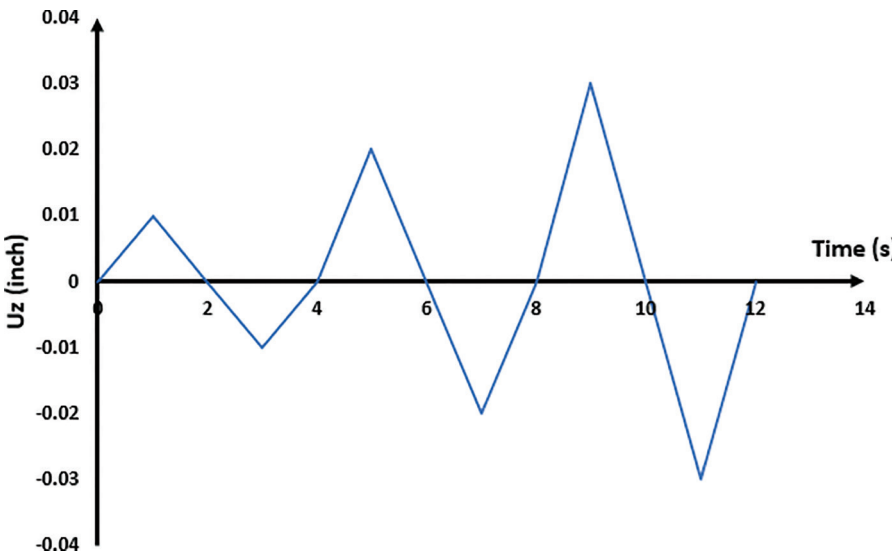

FIGURE 3.6 Displacement loading of the uniaxial test.

3.2 NONLINEAR KINEMATIC HARDENING

3.2.1 Introduction of the Chaboche Model

Under cyclic mechanical loading, the plastic deformation accumulates, and the stress-strain curve has a shift of the stress-strain hysteresis loop along the strain axis (see Figure 3.8), which is called ratcheting. Since the strain in ratcheting increases with the cyclic number of the loading, ratcheting may cause structure failure due

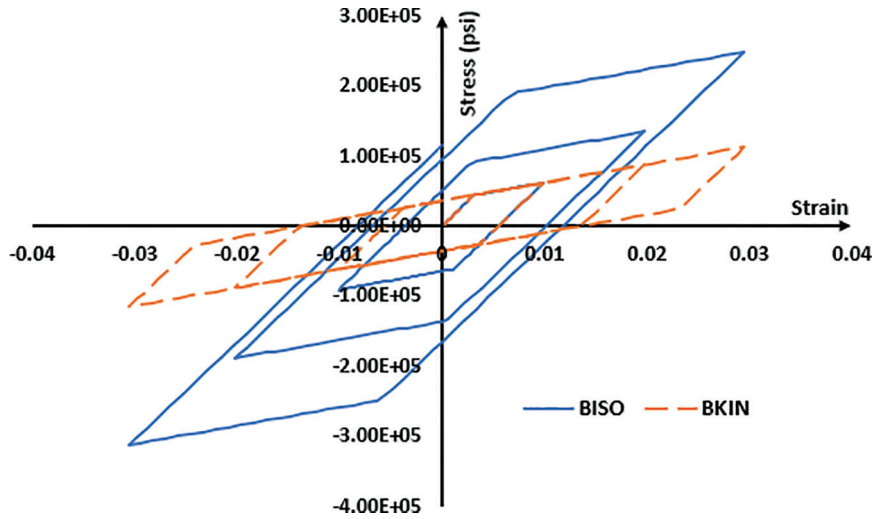

FIGURE 3.7 Stress-strain curves of the BISO and BKIN models under cyclic loading.

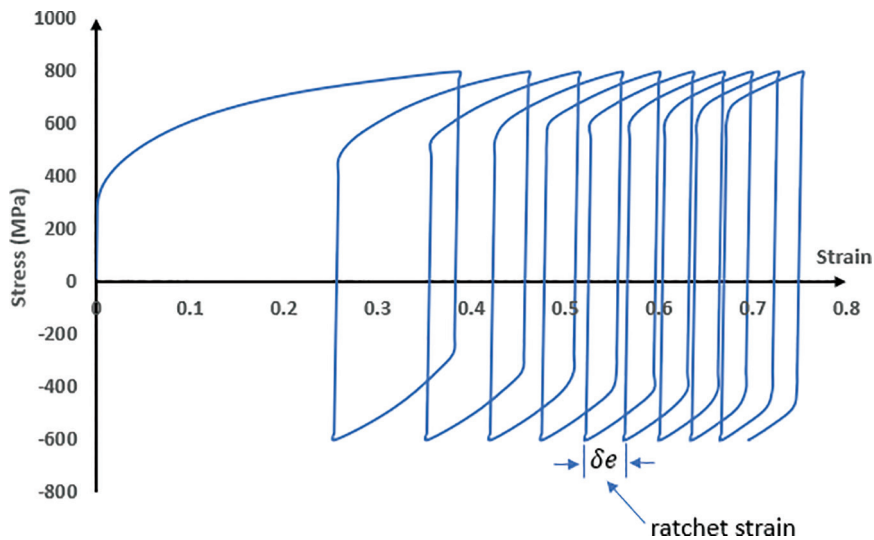

FIGURE 3.8 Ratcheting.

to structural instability; therefore, the study of ratcheting attracts more and more interest. The simulation of ratcheting demands that incremental plastic deformation terms be added to the general cyclic stress-strain equations. Thus, models like the multilinear kinematic hardening model, such as the BKIN and KINH models, cannot predict ratcheting. A few models, including the Chaboche model, are proposed to simulate ratcheting.

Chaboche and Rousselier [3] found that the hardening behavior of the steel material can be better approximated by the sum of various Frederick-Armstrong formulas. The back-stress tensor in the Chaboche model is expressed as

$$\boldsymbol{\alpha} = \sum_{i=1}^{n} \boldsymbol{\alpha}_i \tag{3.5}$$

where n is the number of superposed kinematic models.

The evolution of each back-stress model is specified as

$$\dot{\boldsymbol{\alpha}}_i = \frac{2}{3} C_i \dot{\boldsymbol{\varepsilon}}^{pl} - \gamma_i \dot{\bar{\varepsilon}}^{pl} \boldsymbol{\alpha}_i + \frac{1}{C_i} \frac{dC_i}{d\theta} \theta \dot{\boldsymbol{\alpha}}_i \tag{3.6}$$

where $\dot{\boldsymbol{\varepsilon}}^{pl}$ – plastic strain rate,

$\dot{\bar{\varepsilon}}^{pl}$ – magnitude of the plastic strain rate, and

C_i and γ_i – user-input material parameters.

The Chaboche model is defined in ANSYS using the following commands:

```
TB, Chaboche, 1
TBDATA, 1, σ0
TBDATA,2, C1, γ1
TBDATA, 4, C2, γ2
...
TBDATA, 2n, Cn, γn
```

The Chaboche model can work with any of the available isotropic hardening models. It is very useful for simulating cyclic plastic behavior such as ratcheting.

3.2.2 Curve-Fitting of the Parameters of the Chaboche Model

The n-term Chaboche model has $2n$ parameters that need to be defined before specifying the Chaboche model for modeling. We may achieve it using the curve-fitting tool available in ANSYS. The experimental data come from a low cycle fatigue test [4] (see Figure 3.9). First, the Young's modulus was determined from the elastic stage. Then, the plastic strain was obtained by subtracting the elastic strain from the total strain. With the available data of the plastic strain versus the stress, the curve-fitting was conducted in ANSYS using the following commands:

```
TBFT,EADD,1,UNIA,AMBI.EXP
TBFT,FADD,1,PLAS,CHAB,3 ! THREE-TERM CHABOCHE MODEL

TBFT,SET,1,PLAS,CHAB,3,1,1E6 !INITIALIZE THE PARAMETERS, C1
```

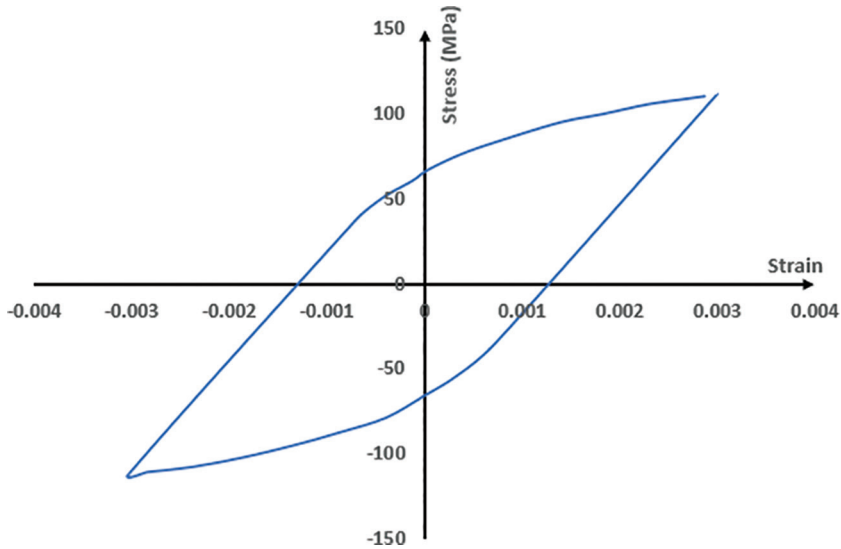

FIGURE 3.9 Experimental data for curve-fitting.

```
TBFT,SET,1,PLAS,CHAB,3,2,1E5 !INITIALIZE THE PARAMETERS, γ1
…

TBFT,SET,1,PLAS,CHAB,3,7,55 !INITIALIZE σ0 = HALF OF  σmax
TBFT,SOLVE,1,PLAS,CHAB,3,0,1000
```

In the above initial value input, σ_0 was defined from half of σ_{max}. Other initial data only chose big values.

Curve-fitting results, which are plotted in Figure 3.10, show that the curve-fitting results effectively match the experimental data. Therefore, the Chaboche model is defined as

```
TB, CHABOCHE, 1, ,3
TBDATA, 1, 67.5
TBDATA, 2, 1.000E+06, 9.371E+04
TBDATA, 4, 1.077E+04, 9.994E+04
TBDATA, 6, 4.110E+04, 1.111E+03
```

3.2.3 Simulation of Ratcheting in a Notched Bar

In this example, a notched bar subjected to cycling loading was simulated to produce the plastic ratchetting in ANSYS190.

3.2.3.1 Finite Element Model

A 2-D axisymmetrical notched rod was modeled in ANSYS190 using Plane182 with keyopt (3)=1 (axisymmetrical) (see Figure 3.11). Also, the model was simplified using the symmetrical condition in the vertical direction.

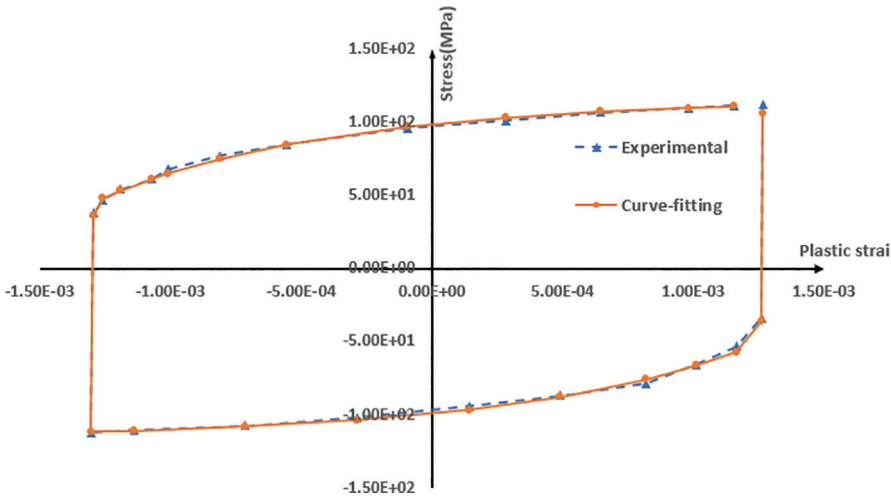

FIGURE 3.10 Curve-fitting results of the Chaboche model.

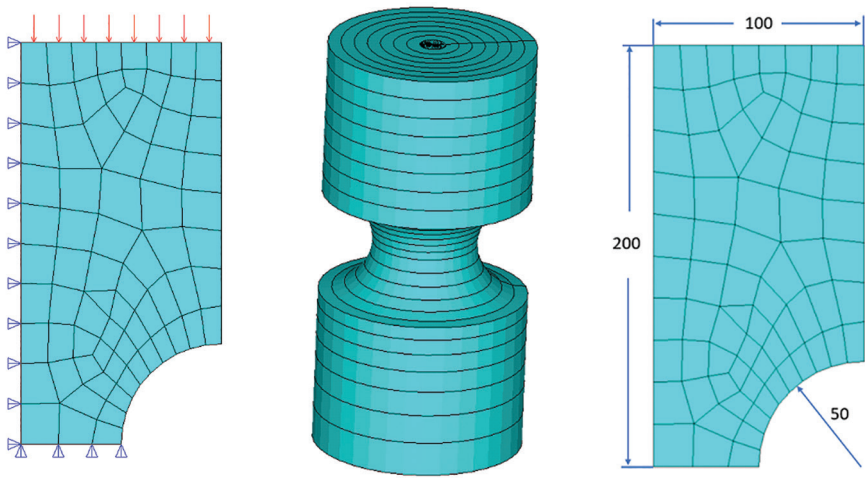

FIGURE 3.11 Finite element model of a notched rod (a) 2-D axisymmetrical, (b) 3-D, and (c) geometry (all dimensions in mm).

3.2.3.2 Material Properties

The rod was defined with the three-term Chaboche model plus the Voce isotropic hardening law (see Table 3.1). The material parameters of the Chaboche model were selected from the curve-fitting results of Section 3.2.

The material model was defined by the following commands:

```
POWER_N=0.1
SIGMA_Y=67.5
TB,NLISO,1,2,5
```

TABLE 3.1
Material Parameters of the Rod [5]

E (MPa)	v	σ_0 (MPa)	C_1	γ_1	C_2	γ_2	C_3	γ_3	n
647,000	0.3	67.5	1e6	9.37e4	1e4	1e5	4.1e4	1.1e3	0.1

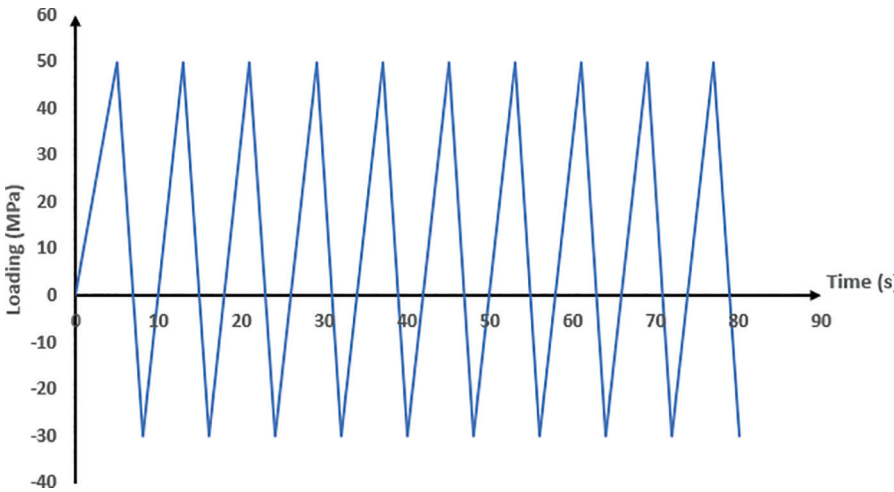

FIGURE 3.12 Loading history.

```
TBDATA,1,SIGMA_Y,POWER_N
TB,CHAB,1,3
TBDATA,1,SIGMA_Y,1E6,9.37E4,1E4,1E5
TBDATA,6,4.1E4,1.1E3
```

For comparison, the model was repeated with the bilinear kinematic hardening model, in which the tangent modulus E_T was chosen for 2,000 MPa.

3.2.3.3 Loadings and Boundary Conditions

The axisymmetrical condition and the symmetrical condition were applied on edges (see Figure 3.11a). The top edge was loaded with ten cycles of loading; each cycle had a maximum of 50 MPa in tension and a minimum of 30 MPa in compression (see Figure 3.12).

3.2.3.4 Results

The von-Mises plastic strain and stress of the rod at the end of the first cycle and the last cycle are plotted in Figures 3.13 and 3.14, respectively. The maximum values occur at the notched tip for both stresses and plastic strains. Comparing the results of the first cycle with those of the last cycle, the stresses do not change much because they are pressure-loaded, but the plastic strains change dramatically between the first and last cycles. Figures 3.15 and 3.16 depict the axial strain versus axial stress

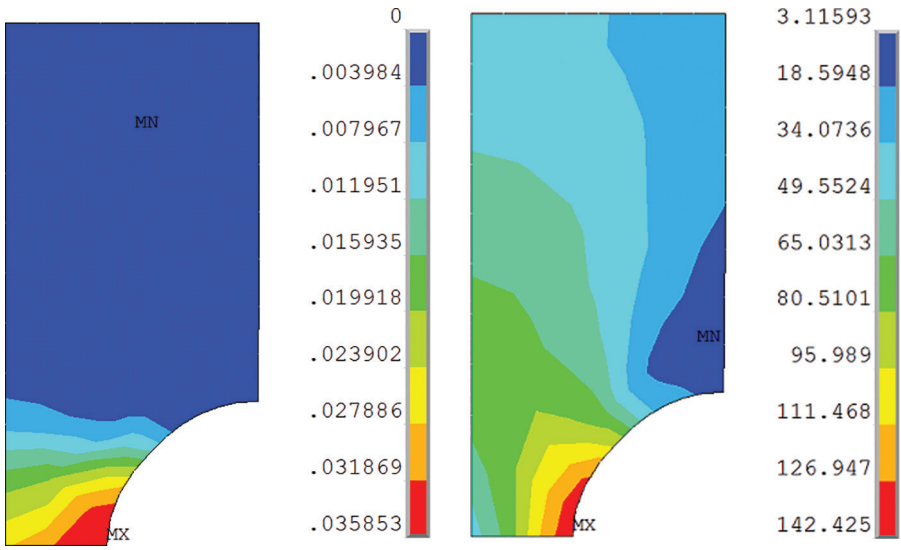

FIGURE 3.13 von-Mises plastic strains and stresses of the rod at the end of the first cycle: (a) von-Mises plastic strains and (b) von-Mises stresses (MPa).

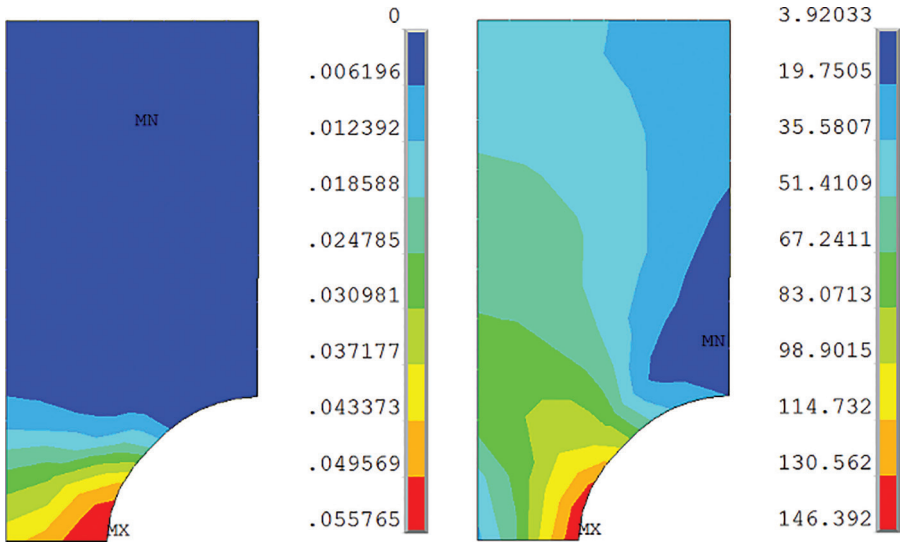

FIGURE 3.14 von-Mises plastic strains and stresses of the rod at the end of the last cycle: (a) von-Mises plastic strains and (b) von-Mises stresses (MPa).

with the Chaboche model and bilinear kinematic hardening model, respectively. Figure 3.15 clearly illustrates a shift of the stress-strain hysteresis loop along the strain axis, which is the ratchetting. On the other hand, no ratchetting appears in Figure 3.16. The difference between Figure 3.15 and Figure 3.16 confirms that the

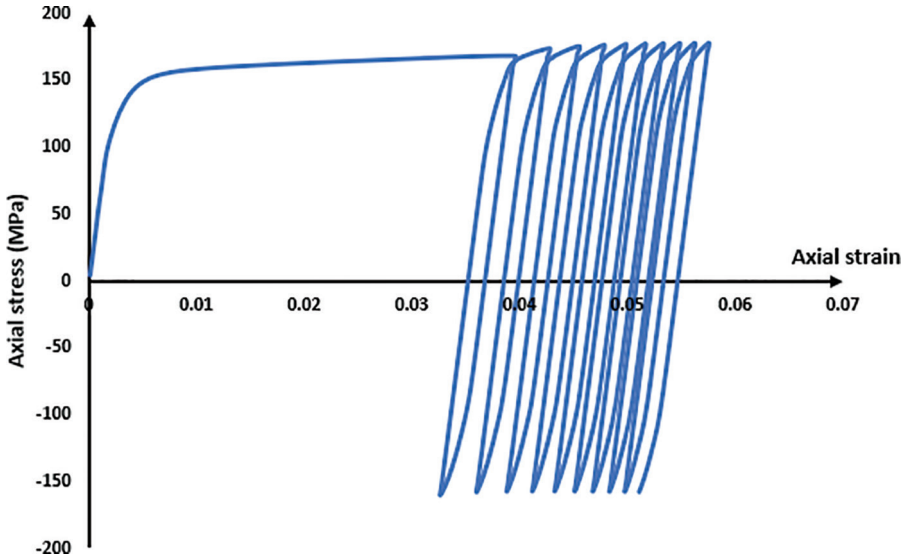

FIGURE 3.15 Axial strain vs axial stress.

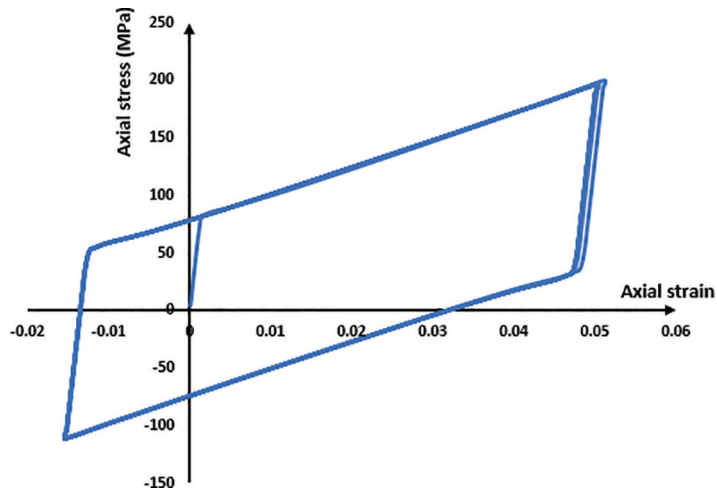

FIGURE 3.16 Axial strain vs axial stress with bilinear kinematic hardening.

ratchetting is modeled by the Chaboche model (nonlinear kinematic hardening), and the bilinear kinematic hardening model cannot produce the ratchetting of metal.

3.2.3.5 Summary

A notched bar with the Chaboche model under cycling loading was studied in ANSYS190. The relation between the axial strain and axial stress reveals the ratchetting due to the Chaboche model (nonlinear kinematic hardening).

REFERENCES

[1] ANSYS190 Help Documentation in the help page of product ANSYS190.
[2] Wang, J.D., and Ohno, N., Two equivalent forms of nonlinear kinematic hardening: application to nonisothermal plasticity, *International Journal of Plasticity*, Vol. 7, 1991, pp. 637–650.
[3] Chaboche, J.L., and Rousselier, G., On the plastic and viscoplastic constitutive equations, Parts I and II, *Journal of Pressure Vessel and Piping*, Vol. 105, 1983, pp. 453–164.
[4] Seisenbacher, B., Winter, G., and Grun, F., Improved approach to determine the material parameters for a combined hardening model, *Material Sciences and Applications*, Vol. 9, 2018, pp. 357–367.
[5] Kang, G., Finite element implementation of advanced constitutive model emphasizing on ratchetting, *18th International Conference on Structural Mechanics in Reactor Technology (SMiRT 18)*, Beijing, China, August 7–12, 2005.